D and D_s decay constants from $N_f = 2 + 1$ lattice QCD

Sara Collins,[a,*] **Jochen Heitger,**[b] **Fabian Joswig,**[c] **Simon Kuberski**[d,e,f] **and Wolfgang Söldner**[a]

[a]*Institut für Theoretische Physik, Universität Regensburg, 93040 Regensburg, Germany.*

[b]*Institut für Theoretische Physik, Universität Münster, Wilhelm-Klemm-Straße 9, 48149 Münster, Germany.*

[c]*Higgs Centre for Theoretical Physics, School of Physics and Astronomy,*
The University of Edinburgh, Edinburgh EH9 3FD, UK.

[d]*Theoretical Physics Department, CERN, 1211 Geneva 23, Switzerland.*

[e]*Helmholtz-Institut Mainz, Johannes Gutenberg-Universität Mainz, Staudingerweg 18,*
55128 Mainz, Germany.

[f]*GSI Helmholtzzentrum für Schwerionenforschung, Planckstraße 1, 64291 Darmstadt, Germany.*
E-mail: sara.collins@ur.de, heitger@uni-muenster.de,
fabian.joswig@ed.ac.uk, simon.kuberski@cern.ch, wolfgang.soeldner@ur.de

The D and D_s decay constants are important inputs for the determination of the CKM matrix elements $|V_{cd}|$ and $|V_{cs}|$ and for precision tests of the Standard Model. With lattice determinations of these quantities reaching the sub-percent level, it is important to demonstrate control over all sources of systematic uncertainty, and in particular, those arising from discretisation effects and the quark mass dependence. We present results obtained from a large number of $N_f = 2 + 1$ CLS ensembles (including two ensembles at the physical point) which span 6 lattice spacings in the range 0.039 fm $\leq a \leq$ 0.1 fm and lie on three trajectories in the quark mass plane.

*Speaker

1. Introduction

Lattice calculations of the charm-light and charm-strange decay constants f_D and f_{D_s}, respectively, together with the experimentally measured decay rates of the weak decays of D and D_s mesons into a lepton and a neutrino can be used to determine the CKM matrix elements $|V_{cd}|$ and $|V_{cs}|$. Such a determination contributes to a wider effort to constrain CKM matrix elements utilising many different processes, enabling precision tests of the unitarity of the matrix to be performed. However, observables involving both charm and light or strange quarks are challenging to compute on the lattice with all sources of systematic uncertainty under control. Discretisation effects arising from the heavy quark action require simulations with fine lattice spacings, while the light (and strange) quark mass dependence needs to be sufficiently constrained, in particular, close to the physical point.

We present results for the decay constants from an analysis of $N_f = 2+1$ Wilson fermion gauge field configurations generated by the Coordinated Lattice Simulations (CLS) consortium [1–3], where the charm quark is introduced as a quenched flavour. For Wilson fermions, the axial-vector matrix elements (through which the decay constants are defined) are multiplicatively renormalised and the action and axial-vector current must be non-perturbatively improved in order to achieve leading order $O(a^2)$ discretisation effects. Nonetheless, employing the precision non-perturbative determination of the renormalisation factor of ref. [4] and the improvement coefficients of refs. [5, 6], renormalisation and improvement are not significant sources of uncertainty in our analysis. In the following, we give details of our lattice setup and the determination of the decay constants on each ensemble. We then outline our approach for performing the continuum and chiral extrapolations and present the final results before summarising. Further details of this analysis can be found in Ref. [7].

2. Lattice setup

We employ 49 high statistics CLS ensembles generated with non-perturbatively $O(a)$ improved Wilson fermions [8, 9] and the tree-level Symanzik improved gauge action [10]. Six lattice spacings are realised with a ranging from 0.098 fm down to 0.039 fm. The ensembles lie on three trajectories in the quark mass plane, as displayed in Fig. 1. Two of the trajectories meet at the physical point: along one trajectory (denoted TrM = const.) the flavour average of the light and strange quark masses is held constant, and along the other (referred to as $\widehat{m}_s \approx$ const.) the strange quark mass is fixed to approximately its physical value. The third trajectory (labelled $m_1 = m_s$) runs towards the SU(3) chiral limit, with the light and strange quark masses set to be equal. Overall, the pion mass varies from $m_\pi \approx 420$ MeV down to 129 MeV, where for most ensembles the spatial extent L is large enough such that $m_\pi L \gtrsim 4$ and significant finite-volume effects are avoided. Lattice spacings as fine as 0.04 fm are achieved utilising open boundary conditions in time [11] to avoid the problem of topological freezing. The charm quark is partially quenched in our analysis. Two values of the charm quark mass are employed per ensemble, which are chosen such that only a small interpolation or (in a few cases) extrapolation to the physical value is required.

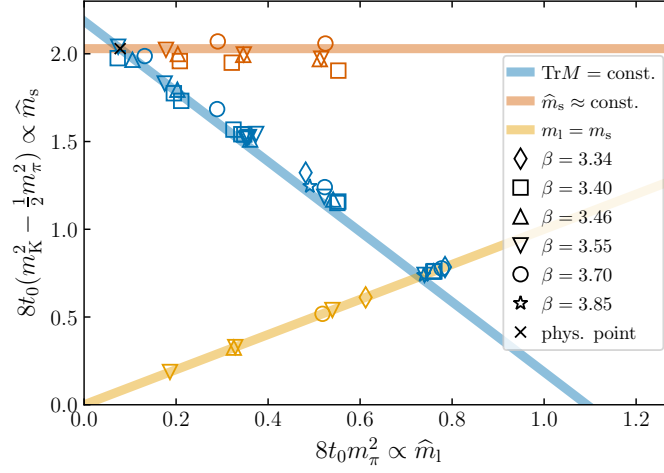The pseudoscalar decay constants f_D and f_{D_s} are defined via the matrix elements of the axial

Figure 1: Overview of the ensembles used in this work in the plane of (renormalised) light and strange quark masses: the chiral trajectory where TrM = const. approaches the physical point from below (blue line) and meets the trajectory with renormalised strange quark mass $\widehat{m}_s \approx$ const. (orange line) at the physical point by construction. A third trajectory for which the light and strange quark masses are equal, $m_l = m_s$ (yellow line), approaches the SU(3) chiral limit. The orange line is obtained by setting $8t_0(m_K^2 - \frac{1}{2}m_\pi^2)$ to its physical value, analogously the blue line is defined by fixing $\bar{\mathbb{M}}^2 \equiv 8t_0\left(2m_K^2 + m_\pi^2\right)/3 = \bar{\mathbb{M}}^2_{\text{phys}}$.

vector current between D and D$_s$ meson states at momentum p and the vacuum, respectively,

$$\left\langle 0\middle|A_\mu^{\text{lc}}\middle|D(p)\right\rangle = \mathrm{i}f_D p_\mu, \qquad \left\langle 0\middle|A_\mu^{\text{sc}}\middle|D_s(p)\right\rangle = \mathrm{i}f_{D_s}p_\mu. \tag{1}$$

The axial vector current is given by $A_\mu^{qc}(x) = \overline{q}(x)\gamma_\mu\gamma_5 c(x)$ for quark flavours $q = l, s$. In order to remove O(a) cutoff effects from the matrix elements, we construct an improved current

$$A_\mu^{qc,\text{I}} = A_\mu^{qc} + ac_A\frac{1}{2}\left(\partial_\mu + \partial_\mu^*\right)P^{qc}, \tag{2}$$

where the pseudoscalar operator is $P^{qc}(x) = \overline{q}(x)\gamma_5 c(x)$ and ∂_μ and ∂_μ^* denote the lattice forward and backward derivatives, respectively. Including the mass dependent $O(a)$ improvement terms, the renormalised improved current reads [12]

$$\left(A_\mu^{qc,\text{I}}\right)_{\text{R}} = Z_A\left[1 + a\left(b_A m_{qc} + \bar{b}_A\text{Tr}M\right)\right]A_\mu^{qc,\text{I}} + \text{O}(a^2), \tag{3}$$

where m_{qc} and TrM denote the bare vector Ward identity quark mass combinations

$$m_{qc} = \frac{1}{2}\left(m_q + m_c\right), \quad \text{Tr}M = 2m_l + m_s, \quad \text{with } m_q = \frac{1}{2a}\left(\frac{1}{\kappa_q} - \frac{1}{\kappa_{\text{crit}}}\right). \tag{4}$$

The hopping parameter for quark flavour q is denoted by κ_q and κ_{crit} labels its critical value. For the renormalisation factor Z_A and the improvement coefficients c_A and b_A, we employ the non-perturbative determinations of refs. [4–6], respectively. The improvement coefficient $\bar{b}_A$ has been computed in refs. [6, 13], however, as the coefficient is compatible with zero for the range of gauge couplings considered here, we set $\bar{b}_A = 0$ in our analysis. For κ_{crit} we utilise the results of Ref. [3].

In order to obtain the matrix elements of eq. (1), we evaluate the two-point functions

$$C_{A_0\tilde{P}}^{qc}(t) \equiv C_{A_0\tilde{P}}^{qc}(x_0, y_0) = -\frac{a^6}{L^3} \sum_{\vec{x}, \vec{y}} \left\langle A_0^{qc,I}(x) \left(\tilde{P}^{qc}(y)\right)^\dagger \right\rangle,$$

$$C_{\tilde{P}\tilde{P}}^{qc}(t) \equiv C_{\tilde{P}\tilde{P}}^{qc}(x_0, y_0) = -\frac{a^6}{L^3} \sum_{\vec{x}, \vec{y}} \left\langle \tilde{P}^{qc}(x) \left(\tilde{P}^{qc}(y)\right)^\dagger \right\rangle, \tag{5}$$

at zero momentum, where $t = x_0 - y_0$ is the difference between the sink and source timeslices, x_0 and y_0, respectively. The spatial extent is denoted by L. The correlators are calculated by means of point-to-all propagators, where, for the pseudoscalar interpolator at the source and sink $\tilde{P}^{qc(\dagger)}$, we apply Wuppertal smearing [14, 15] with APE-smoothed links [16]. The number of smearing iterations is varied across the ensembles in order to optimise the overlap with the ground state. Note that the charm propagators are computed with the highest numerical precision that is possible with our code: we impose relative residuals of around 10^{-15}. No problems due to the numerical accuracy of the charm quark propagators are observed when fitting to the correlation functions to extract the heavy-light meson masses and decay constants (within the fit ranges chosen). In order to increase statistics, the source operators are inserted, for most ensembles, at 20-30 different temporal positions. For the open-boundary ensembles, the two-point correlation functions are only averaged over the source and sink timeslices which lie within the bulk, where translational invariance applies.

We perform a combined fit to the $\tilde{P}\tilde{P}$ and $A_0\tilde{P}$ correlation functions. The fitting range $[t_{\min}, t_{\max}]$ for each correlation function is chosen from an analysis of the corresponding effective mass. The upper end of the fit region is set by the time slice where the relative statistical uncertainty of the effective mass exceeds 8%. The start of the fit region $t_{\min}$ is chosen by performing a two-state fit to the effective mass and applying the criterion that the contribution of the excited states is less than $\frac{1}{4}$ of the statistical uncertainty. In this way, excited state contributions to the two-point functions can be neglected within the fitting range and the correlation functions are modelled with single-exponentials with the same energy m_D for $q = l$, and m_{D_s} for $q = s$ and amplitudes $A_{A_0\tilde{P}}^{qc}$ and $A_{\tilde{P}\tilde{P}}^{qc}$,

$$C_{A_0\tilde{P}}^{qc}(x_0, y_0) = A_{A_0\tilde{P}}^{qc} e^{-m_{D_{(q)}}(x_0-y_0)}, \quad C_{\tilde{P}\tilde{P}}^{qc}(x_0, y_0) = A_{\tilde{P}\tilde{P}}^{qc} e^{-m_{D_{(q)}}(x_0-y_0)}, \tag{6}$$

Based on the spectral decomposition of the correlators, the bare matrix elements are extracted from the ground state energy and amplitudes via

$$f_{D_{(q)}} = \frac{\sqrt{2} A_{A_0\tilde{P}}^{qc}}{\sqrt{A_{\tilde{P}\tilde{P}}^{qc} m_{D_{(q)}}}}. \tag{7}$$

Representative results of the combined fits are displayed in Fig. 2 for the heavy-light meson on ensemble E300 ($m_\pi = 175$ MeV, $a = 0.049$ fm). The right panel compares the result for the decay constant, computed as given in eq. (7), with an effective decay constant constructed from the correlation functions and the fitted meson mass:

$$f_{D_{(q)}}^{\text{eff}}(x_0, y_0) = \frac{\sqrt{2} C_{A_0\tilde{P}}^{qc,I}(x_0, y_0)}{\sqrt{C_{\tilde{P}\tilde{P}}^{qc}(x_0, y_0) m_{D_{(q)}} e^{-m_{D_{(q)}}(x_0-y_0)}}} \tag{8}$$
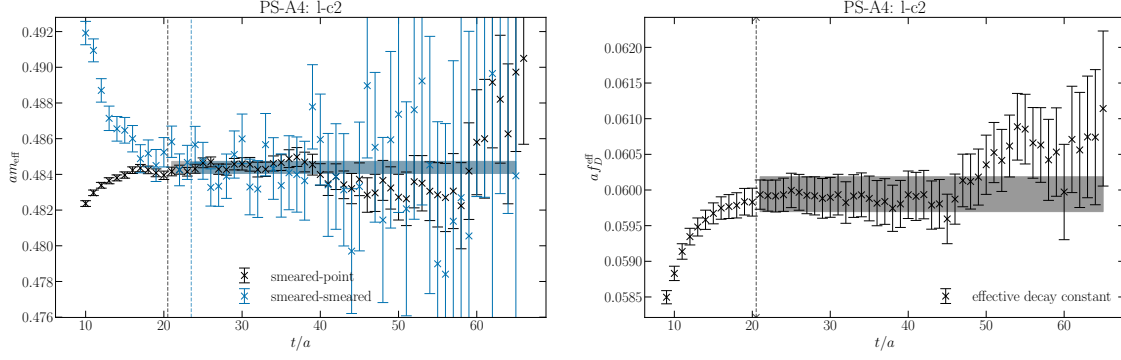
Figure 2: Results from combined fits to the $\tilde{P}\tilde{P}$ and $A_0\tilde{P}$ two-point functions for the heavy-light meson on ensemble E300 ($m_\pi = 175$ MeV, $a = 0.049$ fm). (Left) The fit result for the meson mass (blue band) is shown together with the effective masses of the two correlation functions. The lower end of the fit range ($t_{\min}$) in each case is indicated by a dashed line. (Right) The result for the decay constant obtained from the fit (grey band) is displayed along with the effective decay constant (eq. (8)). The dashed line indicates the $t_{\min}$ of the $A_0\tilde{P}$ two-point function.

We achieve a statistical precision at the level of about 0.5% for $f_{D_{(q)}}$, in most cases. The statistical uncertainties and the (auto-)correlations of the Monte Carlo data are determined and propagated using the Γ-method [17, 18]. We utilise the `pyerrors` package implementation of this method [19].

3. Continuum and chiral extrapolation

We perform a combined fit to the heavy-light and heavy-strange decay constants, which by construction are equal on the ensembles with SU(3) symmetry. The decay constants are evaluated for two values of the heavy quark mass on each ensemble and we fit all the data together, accounting for the heavy quark mass dependence in the fit parametrisation.

We model the dependence of the decay constants on the light, strange and charm quark masses and the lattice spacing using parameterisations of the general form,

$$\sqrt{8t_0}\, f_{D_{(s)}}(m_\pi, m_K, m_{\bar{D}}, a) = \sqrt{8t_0}\, f_{D_{(s)}}^{\mathrm{cont}}(m_\pi, m_K, m_{\bar{D}}, 0) + c_{D_{(s)}}(m_\pi, m_K, m_{\bar{D}}, a), \qquad (9)$$

where we rescale the decay constants with $\sqrt{8t_0}$ so that we fit to dimensionless quantities. The leading terms of the continuum part of the parameterisation are inspired by next-to-leading order (NLO) SU(3) heavy meson chiral perturbation theory (HMχPT) [20]

$$\sqrt{8t_0}\, f_{D_s}^{\mathrm{cont}}(m_\pi, m_K, m_{\bar{D}}, 0) = f_0 + c_1 \bar{\mathbb{M}}^2 + \frac{2}{3}c_2\, \delta\mathbb{M}^2 + c_3\left(4\mu_K + \frac{4}{3}\mu_\eta\right) + c_4\bar{\mathbb{M}}_{\mathrm{H}} + \dots \qquad (10)$$

$$\sqrt{8t_0}\, f_D^{\mathrm{cont}}(m_\pi, m_K, m_{\bar{D}}, 0) = f_0 + c_1 \bar{\mathbb{M}}^2 - \frac{1}{3}c_2\, \delta\mathbb{M}^2 + c_3\left(3\mu_\pi + 2\mu_K + \frac{1}{3}\mu_\eta\right) + c_4\bar{\mathbb{M}}_{\mathrm{H}} + \dots \qquad (11)$$

where

$$\bar{\mathbb{M}}^2 = \frac{8t_0}{3}\left(2m_K^2 + m_\pi^2\right), \quad \delta\mathbb{M}^2 = 16t_0\left(m_K^2 - m_\pi^2\right), \quad \mu_X = 8t_0 m_X^2 \log(8t_0 m_X^2), \qquad (12)$$

5

with X $\in \{\pi, \mathrm{K}, \eta\}$. The mass of the η meson is given by the Gell-Mann-Okubo relation

$$m_\eta^2 \approx \frac{4}{3}m_K^2 - \frac{1}{3}m_\pi^2 = \bar{M}^2 + \frac{1}{3}\delta M^2 \,. \tag{13}$$

Note that SU(3) symmetry constrains the coefficients of the expansion, with $f_\mathrm{D} = f_{\mathrm{D_s}}$ when $\delta M^2 = 0$, and, to this order, only four low energy constants are needed to parameterise both decay constants. The heavy quark mass dependence is modelled using

$$\bar{\mathbb{M}}_\mathrm{H} = \sqrt{8t_0}m_{\bar{\mathrm{D}}}, \quad m_{\bar{\mathrm{D}}} = \left(\frac{2}{3}m_\mathrm{D} + \frac{1}{3}m_{\mathrm{D_s}}\right) \tag{14}$$

After the implementation of $O(a)$ improvement, the leading discretisation terms are

$$c_{\mathrm{D_{(s)}}}(m_\pi, m_K, m_{\bar{\mathrm{D}}}, a) = \mathbb{a}^2(c_{a1} + c_{a2}\bar{\mathbb{M}}^2 + c_{a(3,4)}\delta\mathbb{M}^2 + c_{a5}\bar{\mathbb{M}}_\mathrm{H}) + \dots \tag{15}$$

where $\mathbb{a}^2 = a^2/(8t_0)$, with t_0 determined on each ensemble. For the D (D_s) meson decay constant, the coefficient of the $\delta\mathbb{M}^2$ term is c_{a3} (c_{a4}).

We consider additional terms in the fit form and, by investigating the fit quality, we construct a model with a minimal number of parameters that is able to describe our data reasonably well,

$$\sqrt{8t_0}f_{\mathrm{D_s}}(m_\pi, m_K, m_{\bar{\mathrm{D}}}, a) = f_0 + c_1\bar{\mathbb{M}}^2 + \frac{2}{3}c_2\delta\mathbb{M}^2 + c_3\left(4\mu_K + \frac{4}{3}\mu_\eta\right) \qquad + c_4\bar{\mathbb{M}}_\mathrm{H} \tag{16}$$
$$+ c_5\bar{\mathbb{M}}_\mathrm{H}^2 + c_6\delta\mathbb{M}^2\bar{\mathbb{M}}_\mathrm{H} + c_8\bar{\mathbb{M}}^2\bar{\mathbb{M}}_\mathrm{H} + c_{a1}\mathbb{a}^2 + c_{a5}\mathbb{a}^2\bar{\mathbb{M}}_\mathrm{H},$$
$$\sqrt{8t_0}f_{\mathrm{D}}(m_\pi, m_K, m_{\bar{\mathrm{D}}}, a) = f_0 + c_1\bar{\mathbb{M}}^2 - \frac{1}{3}c_2\delta\mathbb{M}^2 + c_3\left(3\mu_\pi + 2\mu_K + \frac{1}{3}\mu_\eta\right) + c_4\bar{\mathbb{M}}_\mathrm{H}$$
$$+ c_5\bar{\mathbb{M}}_\mathrm{H}^2 + c_7\delta\mathbb{M}^2\bar{\mathbb{M}}_\mathrm{H} + c_8\bar{\mathbb{M}}^2\bar{\mathbb{M}}_\mathrm{H} + c_{a1}\mathbb{a}^2 + c_{a5}\mathbb{a}^2\bar{\mathbb{M}}_\mathrm{H}.$$

Only eleven parameters are needed to describe the 160 naive degrees of freedom, which are effectively reduced due to the correlation in the data (between the masses and decay constants determined on the same ensemble). The fit quality for this fully correlated fit is $\chi^2/\mathrm{d.o.f} = 1.08$. The above expressions remain consistent with SU(3) constraints and there is only one fit parameter (c_6 respectively c_7) that is not shared by the ansätze for f_D and $f_{\mathrm{D_s}}$. To explore the parameter space of the extrapolation further and to test for higher order effects, we build a variety of models, which extend eq. (16). We add up to four terms out of the following list of higher order terms in the quark masses,

$$\bar{\mathbb{M}}^2\bar{\mathbb{M}}_\mathrm{H}^2, \quad \bar{\mathbb{M}}^2\delta\mathbb{M}^2, \quad (\delta\mathbb{M}^2)^2, \quad \delta\mathbb{M}^2\bar{\mathbb{M}}_\mathrm{H}^2, \quad (\delta\mathbb{M}^2)^2\bar{\mathbb{M}}_\mathrm{H}, \tag{17}$$

and up to three terms out of the following lists of terms describing lattice artifacts,

$$\mathbb{a}^2\bar{\mathbb{M}}^2, \quad \mathbb{a}^2\delta\mathbb{M}^2, \quad \mathbb{a}^3, \quad \mathbb{a}^3\bar{\mathbb{M}}^2, \quad \mathbb{a}^3\delta\mathbb{M}^2, \quad \mathbb{a}^3\bar{\mathbb{M}}_\mathrm{H}, \quad \mathbb{a}^4, \quad \mathbb{a}^4\bar{\mathbb{M}}^2, \quad \mathbb{a}^4\delta\mathbb{M}^2, \quad \mathbb{a}^4\bar{\mathbb{M}}_\mathrm{H}. \tag{18}$$

We exclude models that mix a^3 and a^4 cutoff effects and models with more than 16 parameters. In total this amounts to $K = 482$ models. The worst fit quality found in this set has a fully correlated $\chi^2/\mathrm{d.o.f.} = 1.09$. The best fit quality of the models under consideration, $\chi^2/\mathrm{d.o.f.} = 0.92$, is obtained when adding a $\delta\mathbb{M}^2\bar{\mathbb{M}}_\mathrm{H}^2$, $\mathbb{a}^3$ and $\mathbb{a}^3\delta\mathbb{M}^2$ term to eq. (16). This fit is displayed in Fig. 3.
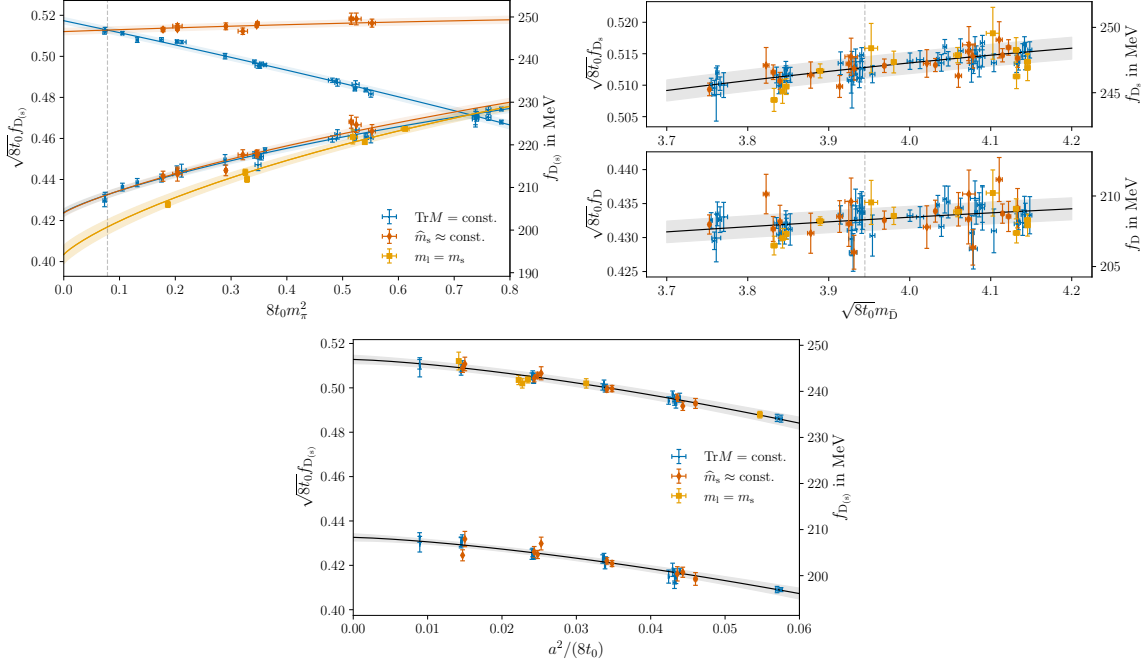
Figure 3: Simultaneous continuum and chiral extrapolation of f_D and f_{D_s} for the parameterisation with the best fit quality. The vertical dashed lines indicate the physical point. The dependence on (top, left) the pion mass squared, (top, right) the flavour average D meson mass and (bottom) the lattice spacing squared is displayed. For the top figures, lattice spacing effects are removed using the fit. For the top-right and bottom plots, the data points are shifted to the physical pion and kaon masses and for the latter and the top-left plot the data are shifted to the physical $\bar{D}$ meson mass.

Starting with the light quark mass dependence, the data lie along the three trajectories: the $\mathrm{Tr}M = $ const. and $\widehat{m}_s \approx $ const. trajectories (blue and red data points and fit curves, respectively) have to coincide by definition at the physical point, tightly constraining the fit. The fit curves clearly show that the strange quark effects on f_D are small, while f_{D_s} is largely insensitive to the light quark mass, when keeping the strange quark mass at its physical value. Along the symmetric line (yellow data points and curve), which approaches the SU(3) chiral limit when lowering the pion mass, the f_D and f_{D_s} decay constants are equal. The curvature due to the chiral logarithms can be mapped out thanks to the two ensembles at physical pion mass and several further ensembles with $m_\pi < 200$ MeV. Turning to the heavy quark mass dependence, shown in the top-right plot in Fig. 3, we see that the results bracket the physical value of the flavour average D meson mass. By performing a global fit of the heavy quark mass dependence, we are able to resolve terms quadratic in $\bar{\mathbb{M}}_H$. However, as seen in the figure, these contributions are rather minor.

Discretisation effects are a significant source of systematics for observables involving charm quarks, with $am_c \approx 0.6$ for our coarsest lattice spacing. However, by utilising high statistics data at six lattice spacings ranging from $a \approx 0.10$ fm down to $a = 0.039$ fm (a^2 varies by more than a factor of 6), we are able to clearly resolve the lattice spacing dependence, including both $\mathtt{a}^2$ and $\mathtt{a}^3$ terms. Figure 3 shows that with full non-perturbative O(a) improvement, the size of these effects is fairly moderate with a 5% difference between the decay constants at the coarsest lattice spacing

and in the continuum limit.

4. Results

We extract results for the decay constants f_{D_s} and f_D at the physical point (in the continuum limit) in physical units for each of the 482 fits considered. For this purpose, we employ the physical value of the flow scale of Ref. [3] and define the physical point in isospin symmetric QCD using the values for the pion and kaon masses given in FLAG's 2016 review [21], $m_\pi = 134.8(3)$ MeV and $m_K = 494.2(3)$ MeV. Utilising the isospin corrected masses of the D and D_s mesons quoted in Ref. [22], we take flavour average D meson mass at the physical point to be $m_{\bar{D}} = 1899.4(3)$ MeV. For the ratio f_{D_s}/f_D, we simply divide the results at the physical point for the individual decay constants. As our simultaneous fits to f_D and f_{D_s} take all correlations into account, we would not expect to obtain more precise results by fitting to the ratio. Performing a model averaging procedure based on the Akaike information criterion (AIC) [23, 24], our final results read

$$
\begin{aligned}
f_{D_s} &= 246.8(0.64)_{\text{stat}}(0.61)_{\text{sys}}(0.95)_{\text{scale}}[1.3]\,\text{MeV}\,, \\
f_D &= 208.4(0.67)_{\text{stat}}(0.75)_{\text{sys}}(1.11)_{\text{scale}}[1.5]\,\text{MeV}\,, \\
f_{D_s}/f_D &= 1.1842(21)_{\text{stat}}(22)_{\text{sys}}(19)_{\text{scale}}[36]\,,
\end{aligned}
\tag{19}
$$

where the first error is statistical, the second is due to the systematics and the third arises from the scale setting. The statistical error includes the uncertainties due to the renormalisation and improvement coefficients and the hadronic scheme, while the systematic error quantifies the uncertainty stemming from the model variation for continuum and quark mass extrapolations or interpolations. The total uncertainty obtained by adding the individual errors in quadrature is given within the square brackets. The uncertainty due to the scale setting dominates the total in the case of f_D and f_{D_s} and contributes to the error of the ratio via the definition of the physical point. The systematic uncertainties are of a similar size as the statistical uncertainties, where the former is mostly due to the uncertainty arising from the continuum limit extrapolation.

In figure 4, we compare our values with recent $N_f = 2 + 1$ and $N_f = 2 + 1 + 1$ determinations. Only those results that consider all sources of systematic uncertainty in their analysis and pass the quality criteria of the FLAG 21 review [25] (for the continuum limit, chiral and finite volume extrapolations, renormalisation and the treatment of the heavy quark) are shown. We also only display the latest results for each collaboration. Note that the ALPHA 23 study of Ref. [26] utilises a small subset of the ensembles employed in the present analysis and we expect some statistical correlation with our values. For the $N_f = 2 + 1$ theory, our results are the most precise and represent a significant improvement on earlier studies. All works are in reasonable agreement with each other. FNAL/MILC [27] quote the smallest total uncertainties of around $0.3(0.2)\%$ for $f_D(f_{D_s})$ and 0.1% for f_{D_s}/f_D, and their results dominate the FLAG average for $N_f = 2 + 1 + 1$. At this level of precision, the definition of isospin symmetric QCD has a significant impact on the values of the decay constants. The FNAL/MILC results for the individual decay constants lie roughly 2σ above ours, while the results for the ratio are slightly more consistent.
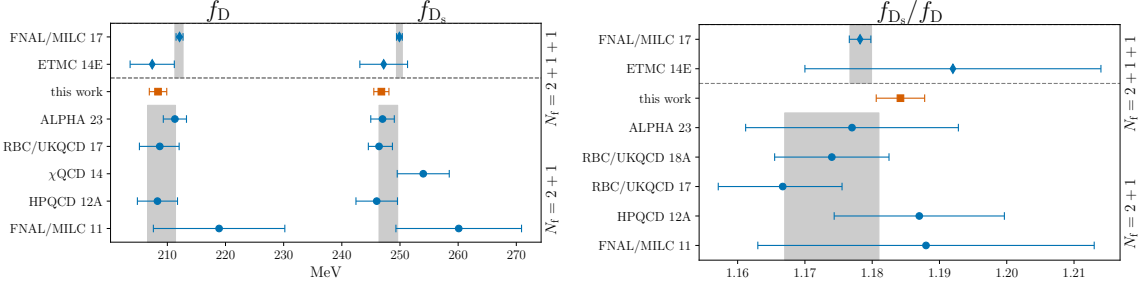
Figure 4: Comparison of lattice results for the decay constants f_D and f_{D_s} (top) and their ratio (bottom) for $N_f = 2 + 1$ [26, 28–33] and $N_f = 2 + 1 + 1$ [27, 34]. Only results that fulfil all the FLAG quality criteria and that are not superseded by later works are displayed. The grey bands show the FLAG 21 averages from Ref. [25].

5. Summary and outlook

We determine the leptonic decay constants of the D and D_s mesons in $2 + 1$ flavour lattice QCD with Wilson fermions. Utilising a large number of high statistics ensembles at six values of the lattice spacing, which lie on three distinct quark mass trajectories covering a wide range of light and strange quark masses enables us to achieve an excellent description of both the cutoff effects and the quark mass dependence down to the physical point. We achieve a 0.5%, 0.7% and 0.3% overall error in f_{D_s}, f_D and f_{D_s}/f_D, respectively. These are the most precise $2 + 1$ flavour results to-date. Further improvement in the determination of the decay constants would require a more precise evaluation of the scale, followed by a reduction in both the statistical and systematic errors. However, once the uncertainties are reduced to the level of a few per mille, isospin-breaking effects, as well as the absence of charm sea quarks, will need to be considered.

References

[1] M. Bruno et al., *Simulation of QCD with $N_f = 2 + 1$ flavors of non-perturbatively improved Wilson fermions*, *JHEP* **02** (2015) 043 [`1411.3982`].

[2] D. Mohler, S. Schaefer and J. Simeth, *CLS 2+1 flavor simulations at physical light- and strange-quark masses*, *EPJ Web Conf.* **175** (2018) 02010 [`1712.04884`].

[3] RQCD collaboration, *Scale setting and the light baryon spectrum in $N_f = 2 + 1$ QCD with Wilson fermions*, *JHEP* **05** (2023) 035 [`2211.03744`].

[4] M. Dalla Brida, T. Korzec, S. Sint and P. Vilaseca, *High precision renormalization of the flavour non-singlet Noether currents in lattice QCD with Wilson quarks*, *Eur. Phys. J. C* **79** (2019) 23 [`1808.09236`].

[5] ALPHA collaboration, *Non-perturbative improvement of the axial current in N_f=3 lattice QCD with Wilson fermions and tree-level improved gauge action*, *Nucl. Phys.* **B896** (2015) 555 [`1502.04999`].

[6] RQCD collaboration, *Masses and decay constants of the η and η' mesons from lattice QCD*, *JHEP* **08** (2021) 137 [`2106.05398`].

[7] S. Kuberski, F. Joswig, S. Collins, J. Heitger and W. Söldner, D *and* D_s *decay constants in* $N_f = 2 + 1$ *QCD with Wilson fermions*, `2405.04506`.

[8] B. Sheikholeslami and R. Wohlert, *Improved Continuum Limit Lattice Action for QCD with Wilson Fermions*, *Nucl. Phys.* **B259** (1985) 572.

[9] J. Bulava and S. Schaefer, *Improvement of $N_f = 3$ lattice QCD with Wilson fermions and tree-level improved gauge action*, *Nucl. Phys.* **B874** (2013) 188 [`1304.7093`].

[10] M. Lüscher and P. Weisz, *On-Shell Improved Lattice Gauge Theories*, *Commun. Math. Phys.* **97** (1985) 59.

[11] M. Lüscher and S. Schaefer, *Lattice QCD without topology barriers*, *JHEP* **07** (2011) 036 [1105.4749].

[12] T. Bhattacharya, R. Gupta, W. Lee, S. R. Sharpe and J. M. S. Wu, *Improved bilinears in lattice QCD with non-degenerate quarks*, *Phys. Rev. D* **73** (2006) 034504 [hep-lat/0511014].

[13] P. Korcyl and G. S. Bali, *Non-perturbative determination of improvement coefficients using coordinate space correlators in $N_f = 2 + 1$ lattice QCD*, *Phys. Rev. D* **95** (2017) 014505 [1607.07090].

[14] S. Güsken, U. Löw, K. Mütter, R. Sommer, A. Patel and K. Schilling, *Nonsinglet Axial Vector Couplings of the Baryon Octet in Lattice QCD*, *Phys. Lett.* **B227** (1989) 266.

[15] S. Güsken, *A Study of smearing techniques for hadron correlation functions*, *Nucl. Phys. B Proc. Suppl.* **17** (1990) 361.

[16] M. Falcioni, M. Paciello, G. Parisi and B. Taglienti, *Again on SU(3) glueball mass*, *Nucl. Phys.* **B251** (1985) 624.

[17] ALPHA collaboration, *Monte Carlo errors with less errors*, *Comput. Phys. Commun.* **156** (2004) 143 [hep-lat/0306017].

[18] A. Ramos, *Automatic differentiation for error analysis of Monte Carlo data*, *Comput. Phys. Commun.* **238** (2019) 19 [1809.01289].

[19] F. Joswig, S. Kuberski, J. T. Kuhlmann and J. Neuendorf, *pyerrors: A python framework for error analysis of Monte Carlo data*, *Comput. Phys. Commun.* **288** (2023) 108750 [2209.14371].

[20] J. L. Goity, *Chiral perturbation theory for SU(3) breaking in heavy meson systems*, *Phys. Rev.* **D46** (1992) 3929 [hep-ph/9206230].

[21] Flavour Lattice Averaging Group (FLAG) collaboration, *Review of lattice results concerning low-energy particle physics*, *Eur. Phys. J. C* **77** (2017) 112 [1607.00299].

[22] G. S. Bali, S. Collins, A. Cox and A. Schäfer, *Masses and decay constants of the $D_{s0}^*(2317)$ and $D_{s1}(2460)$ from $N_f = 2$ lattice QCD close to the physical point*, *Phys. Rev. D* **96** (2017) 074501 [1706.01247].

[23] H. Akaike, *A new look at the statistical model identification*, *IEEE Transactions on Automatic Control* **19** (1974) 716.

[24] H. Akaike, *Information theory and an extension of the maximum likelihood principle*, in *Springer Series in Statistics*, p. 199, Springer New York, (1998), DOI.

[25] Flavour Lattice Averaging Group (FLAG) collaboration, *FLAG Review 2021*, *Eur. Phys. J. C* **82** (2022) 869 [2111.09849].

[26] ALPHA collaboration, *Hadronic physics from a Wilson fermion mixed-action approach: Charm quark mass and $D_{(s)}$ meson decay constants*, 2309.14154.

[27] FERMILAB LATTICE, MILC collaboration, *B- and D-meson leptonic decay constants from four-flavor lattice QCD*, *Phys. Rev. D* **98** (2018) 074512 [1712.09262].

[28] HPQCD collaboration, *Update: Precision D_s decay constant from full lattice QCD using very fine lattices*, *Phys. Rev. D* **82** (2010) 114504 [1008.4018].

[29] FERMILAB LATTICE, MILC collaboration, *B- and D-meson decay constants from three-flavor lattice QCD*, *Phys. Rev. D* **85** (2012) 114506 [1112.3051].

[30] HPQCD collaboration, *|V_{cd}| from D Meson Leptonic Decays*, *Phys. Rev. D* **86** (2012) 054510 [1206.4936].

[31] χQCD collaboration, *Charm and strange quark masses and f_{D_s} from overlap fermions*, *Phys. Rev. D* **92** (2015) 034517 [1410.3343].

[32] RBC/UKQCD collaboration, *The decay constants $\mathbf{f_D}$ and $\mathbf{f_{D_s}}$ in the continuum limit of $\mathbf{N_f = 2 + 1}$ domain wall lattice QCD*, *JHEP* **12** (2017) 008 [1701.02644].

[33] RBC/UKQCD collaboration, *SU(3)-breaking ratios for $D_{(s)}$ and $B_{(s)}$ mesons*, 1812.08791.

[34] ETM collaboration, *Leptonic decay constants f_K, f_D, and f_{D_s} with $N_f = 2 + 1 + 1$ twisted-mass lattice QCD*, *Phys. Rev. D* **91** (2015) 054507 [1412.7908].

[35] Jülich Supercomputing Centre, *JUWELS: Modular Tier-0/1 Supercomputer at the Jülich Supercomputing Centre*, *J. of large-scale research facilities* **5** (2019) A135.

[36] Jülich Supercomputing Centre, *JURECA: Modular supercomputer at Jülich Supercomputing Centre*, *J. of large-scale research facilities* **4** (2018) A132.

[37] H. Baier et al., *QPACE: A QCD parallel computer based on Cell processors*, *PoS* **LAT2009** (2009) 001 [0911.2174].

[38] Y. Nakamura, A. Nobile, D. Pleiter, H. Simma, T. Streuer, T. Wettig et al., *Lattice QCD Applications on QPACE*, 1103.1363.

[39] SCIDAC, LHPC, UKQCD collaboration, *The Chroma software system for lattice QCD*, *Nucl. Phys. Proc. Suppl.* **140** (2005) 832 [hep-lat/0409003].

[40] M. Lüscher and S. Schaefer. http://luscher.web.cern.ch/luscher/openQCD/.

[41] S. Heybrock, M. Rottmann, P. Georg and T. Wettig, *Adaptive algebraic multigrid on SIMD architectures*, *PoS* **LATTICE2015** (2016) 036 [1512.04506].

[42] T. Korzec. https://github.com/to-ko/mesons.